



Identification of Yld2000–2d anisotropic yield function parameters from single hole expansion test using machine learning

Jinjae Kim^a, Abrar S. Ebrahim^b, Brad L. Kinsey (2)^b, Jinjin Ha^{b,*}

^a Department of Automotive Engineering, Yeungnam University, Republic of Korea

^b Department of Mechanical Engineering, University of New Hampshire, USA

ARTICLE INFO

Article history:

Available online xxx

Keywords:

Machine learning

Sheet metal

Anisotropic yield function parameter

ABSTRACT

This study presents a novel machine learning approach for predicting the anisotropic parameters of the Yld2000–2d non-quadratic yield function using a hole expansion test. Heterogeneous stress-strain fields during the test substitute for multiple experiments required in the conventional parameter identification approach. An artificial neural network model for the parameter prediction is developed using a virtually generated training dataset composed of strains from hole expansion simulations, performed using randomly selected anisotropic parameters. The developed model predicts the Yld2000–2d parameters for AA6022-T4 based on the measured strain field from a hole expansion experiment, and the parameter results are evaluated by comparing anisotropy in uniaxial tension tests, the yield locus, and thinning variation in hole expansion test.

© 2024 CIRP. Published by Elsevier Ltd. All rights reserved.

1. Introduction

Finite element (FE) analysis is often employed to investigate issues in metal forming processes, such as shape irregularities and part failure, prior to implementation in mass production. One of the crucial requirements for the FE simulation is an accurate description of material behavior including the anisotropy during plastic deformation. Among the several anisotropic yield functions proposed over the decades, the Yld2000–2d non-quadratic anisotropic yield function, developed by Barlat et al. [1], has been widely used to describe various levels of plastic anisotropy in different materials, such as aluminum, steel, titanium, etc. The model prediction is often very sensitive to the anisotropic parameters determined by the calibration method. Also, the ability to predict all anisotropy characteristics, e.g., normalized yield stresses and r-values in different orientations, with a single set of anisotropic parameters is challenging and depends on choice of experiments and optimization method [2–4].

Conventionally, the calibration of the anisotropic parameters requires multiple experiments employing specific stress states and material orientations. For instance, the 8 anisotropic parameters of the Yld2000–2d yield function are typically determined by uniaxial tension (UT) in the rolling (RD), diagonal (DD, 45° from the RD), and transverse directions (TD) and a balanced biaxial tension experiments [1]. Additionally, plane-strain tension (PST) or simple shear experiments are used when they are important stress states in the FE analysis. For instance, Park et al. [5] investigated the influence of calibration for accurate description of plastic anisotropy and found that calibration of Yld2000–2d yield function using PST in RD and TD rather than balanced biaxial tension can significantly improve the accuracy of

thickness prediction in hole expansion (HE) tests. To mitigate the substantial costs and efforts associated with these experiments, non-standard testing specimens have been developed to derive anisotropic parameters by inducing heterogeneous deformation incorporating holes, notches, and M-shaped uniaxial or biaxial loading samples [2,6–8]. The heterogeneous strain field can be observed through optical full-field techniques, such as digital image correlation (DIC) [6].

To calibrate the anisotropic parameters from the heterogeneous deformation fields, an inverse method is often used. Finite element model update (FEMU), a popular inverse method, compares the heterogeneous deformation field of FE simulation with the DIC measurements and iteratively updates the yield function parameters until a convergence criterion is satisfied. Several researchers have employed FEMU for anisotropic parameter calibration. Zhang et al. [4] identified the 13 parameters for the Bron and Besson yield function using FEMU. Similarly, Guner et al. [6] described the anisotropy of AA6016-T4 using the Yld2000–2d anisotropic yield function with 8 parameters identified via the FEMU method. Zhang et al. [9] integrated an identifiability framework along with the FEMU process. This allowed them to optimize a notched tensile specimen to enhance the inhomogeneity of the strain field while calibrating the Yld2000–2d anisotropic parameters. However, the FEMU process may need excessive time and computation costs due to the iteration required.

Alternatively, the virtual field method (VFM) was introduced by Rossi and Piuron to address the drawbacks of FEMU [10]. They applied VFM to calibrate the Hill48 yield function parameters. Rossi et al. [11] simultaneously calibrated Hill48 and Yld2000–2d yield function parameters along with the Swift hardening model using a notched specimen. Even though they yielded reasonable results, they suggested specimen geometry optimization for potential improvement.

Wessel et al. [12] recently introduced a machine learning-based sampling in a crystal plasticity FE method to efficiently sample virtual

* Corresponding author.

E-mail address: jinjin.ha@unh.edu (J. Ha).

experiments and identify anisotropic parameters for various anisotropic yield functions. Karadogan et al. [13] applied an artificial neural network (ANN) to determine the 3 parameters of the Yld89 anisotropic yield function. They used 1080 strain values extracted from certain elements of notched tensile sample simulations along 3 orientations as inputs in the ANN model to include various strain fields. However, a complex architecture with many inputs can be a barrier to create an effective ANN model.

In this paper, a feedforward ANN is proposed to predict the Yld2000–2d yield function parameters for AA6022-T4 using a single HE test. In [Section 2](#), material properties and the plasticity model are summarized. [Section 3](#) describes the machine learning strategy, including the virtual training data generation and optimized architecture. [Section 4](#) shows the validation of the developed model comparing plastic anisotropy in UT tests, yield locus, and HE test thinning predictions. [Section 5](#) summarizes conclusions and future work.

2. Material properties and plasticity model

The material used in this study is a 1 mm thick, AA6022-T4 sheet. The material characteristics, including strain hardening and plastic anisotropy, were studied by Ha et al. [3]. UT tests at every 30° from RD to TD, PST tests in the RD, DD, and TD, and a disc compression (DC) test to determine the in-plane strain ratio in balanced biaxial tension were performed. The mechanical properties are summarized in [Table 1](#). Note that a total of 11 data from 8 experiments with 3 different test setups were used to achieve varying stress states to calibrate the Yld2000–2d anisotropic parameters in [3].

Table 1
Summary of mechanical properties of AA6022-T4 [3].

Elastic properties			
Young's modulus	E= 70 GPa	Poisson's ratio	$\nu= 0.3$
Plastic properties ($W^p= 20 \text{ MJ/m}^3$)			
UT	RD	30°	60°
$\sigma/\bar{\sigma}$	1.000	1.016	0.976
r-value	0.793	0.465	0.352
PST	RD	45°	90°
$\sigma/\bar{\sigma}$	1.096	1.019	0.978
DC	r_b	1.080	

In this work, the same Voce isotropic strain hardening model is used as in the previous study [3]:

$$\bar{\sigma} = 430.52 - 213.71 \cdot \exp(-8.88\bar{\varepsilon}) \text{ (MPa)} \quad (1)$$

where $\bar{\varepsilon}$ is the equivalent plastic strain.

The Yld2000–2d non-quadratic anisotropic yield function with a plane-stress condition [1] is used:

$$|X'_1 - X'_2|^m + |2X''_2 + X''_1|^m + |2X''_1 + X''_2|^m = 2\bar{\sigma}^m \quad (2)$$

where $X'_{i=1,2}$ and $X''_{j=1,2}$ are the principal values of two linearly transformed deviatoric stress tensors with anisotropic parameters, i.e., α_{1-8} . An exponent m is recommended to be 6 for body-centered (BCC) and 8 for face-centered cubic (FCC) crystal structure metals, such as AA6022-T4 used in this study. Detailed information regarding this yield function can be found in [1].

3. Machine learning strategy

3.1. Hole expansion simulations

Past research [2,4,6–11] recommends various experiments and non-standard geometries to achieve heterogeneous deformation fields for anisotropic yield function parameter calibration. As an alternative, the HE test achieves various stress states in a single experiment from uniaxial to biaxial tensions along the radial direction of the specimen [3,14]. In this version of the HE test, a cylindrical shaped punch with a recession in the center is used to avoid contact between the punch and the blank near the expanding hole as seen in

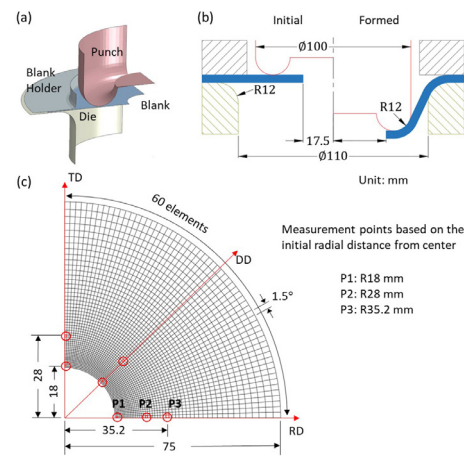


Fig. 1. FE model for hole expansion test: (a) iso-view of quarter model, (b) tool dimensions, and (c) blank mesh with data extraction points.

Fig. 1. The HE test is performed until the first rupture is visually observed in the DIC images.

A HE simulation is performed in ABAQUS/Implicit with the von Mises yield function initially to observe the stress states during the deformation. A schematic of the HE test FE model and meshed quarter blank of 75 mm radius with an initial hole of 17.5 mm radius are shown in [Fig. 1](#). The mesh is generated using element type S4R with 9 integration points through the thickness and 60 elements in circumferential and radial directions. A Coulomb friction coefficient, $\mu= 0.12$, is used.

Stress states are extracted from the elements, which are at the hole edge, i.e., at 17.5 mm, to 34.1 mm in the radial direction on the blank from RD (x-direction) to TD (y-direction). Although the hole will be expanding, the initial element locations will be used to identify these elements during analyses. The measurement points on the mesh and the corresponding stress states with the von Mises yield surface are shown in [Figs. 2\(a\) and \(b\)](#), respectively. Note that the same color indicates the same radial distance from the center. It can be seen that the blank is subjected to various stress states from UT to biaxial tension, including PST. Thus, the HE test in a single experiment provides the various stress states required to predict the anisotropic parameters for the Yld2000–2d yield function.

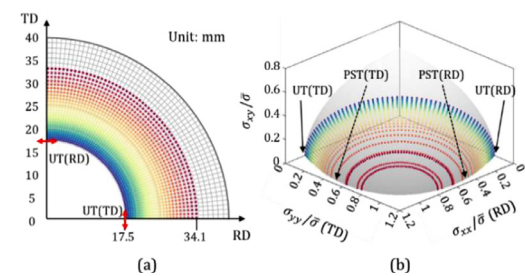


Fig. 2. Stress state analysis from HE simulation: (a) color-coded locations on the mesh and (b) stress states corresponding to color points for von Mises yield surface.

3.2. Virtual training data generation

The HE simulations are performed by implementing a user-defined material subroutine (UMAT) for the Yld2000–2d yield function into ABAQUS/Implicit to virtually generate training data. In total, 2500 simulations are conducted using randomly selected anisotropic parameters between 0.8 and 1.2, i.e., $\alpha_{1-8}=[0.8-1.2]$.

The 2 normal strain components, i.e., ε_{xx} and ε_{yy} , are extracted from 7 elements at certain locations on the specimen (see [Fig. 1\(c\)](#)) and used to train the ANN model for the Yld2000–2d anisotropic parameter prediction. In RD, the data is extracted from 3 elements located initially at 18 mm, 28 mm, and 35.2 mm in the radial direction from the hole center corresponding to UT, PST, and nearly balanced biaxial tension. In DD and TD, the same data is extracted from 2 elements in each direction initially at 18 mm and 28 mm near the

UT and PST. The data initially at 35.2 mm from the center is not included in DD and TD because the nearly balanced biaxial tension would be redundant and bias the ANN training if considered for all 3 directions, i.e., RD, DD, and TD.

3.3. Artificial neural network modelling

The architecture of the ANN model is constructed with the extracted strain data from the simulations and anisotropic parameters as the input and output variables, respectively: 14 normal strain components from the 7 points, i.e., $(\varepsilon_i^{RD1}, \varepsilon_i^{RD2}, \varepsilon_i^{RD3}, \varepsilon_i^{DD1}, \varepsilon_i^{DD2}, \varepsilon_i^{TD1}, \varepsilon_i^{TD2})_{i=xx,yy}$ (see Fig. 1(c)), at a punch stroke of 16 ± 0.005 mm for input and 8 anisotropic parameters of the Yld2000–2d, i.e., α_{1-8} , for output. The datasets are extracted from 2500 simulations and divided into 70 %:15 %:15 % for training, validation, and testing of the model.

KerasTuner, hyperparameter optimization library with random search algorithm, is used to determine the architecture from the training data, with the search space being 2 to 5 hidden layers and 8 to 64 nodes in each layer. The optimal architecture consists of 3 hidden layers with 24, 16 and 8 nodes respectively (see Fig. 3). All hidden layers are activated with the sigmoid function and mean absolute error (MAE) is employed as the loss function. The ANN model is trained in full batch mode with a learning rate of 0.001. Early stopping call back with a patience of 20 is employed to automatically stop and to prevent underfitting or overfitting. The ANN model is successfully trained with MAEs of 0.057, 0.059 and 0.057 for training, validation, and testing, respectively.

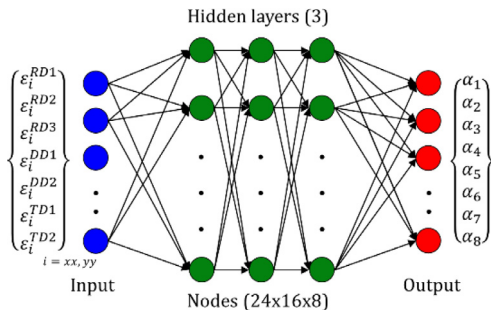


Fig. 3. Architecture of ANN model to predict Yld2000–2d anisotropic parameters.

4. Prediction and validation of Yld2000–2d parameters

4.1. ANN model prediction of Yld2000–2d anisotropic parameters

To predict the Yld2000–2d anisotropic parameters using the ANN model developed in the previous section, the same 14 normal strain data at the 7 locations in Fig. 1(c) from an experimental HE test of AA6022-T4 are used as inputs into the ANN model. The DIC post-processing parameters are 5 for the filter, 29 pixels for the subset, and 1 pixel for the step sizes. The predicted anisotropic parameters are summarized in Table 2 (ANN) with the reference values (Ref.), which were identified by a conventional method using the multiple experiments indicated in Table 1 [3]. Recall that the Ref. parameters were calibrated by a numerical optimization, i.e., least square error minimization, from 8 experiments with 3 different test setups to achieve varying stress states (Table 1) [3] as opposed to the single experiment for the ANN model. The mean deviation of anisotropic parameter values between the Ref. and ANN predictions is 3.13 %, with only one exceeding 3.8 % deviation from the Ref. The ANN prediction for Yld2000–2d parameters is evaluated by two different methods in this paper. Firstly, the plastic anisotropy in the UT tests, i.e., normalized yield stresses and r-values, and yield loci will be

Table 2

Yld2000–2d anisotropic parameters for AA6022-T4 ($m = 8$).

	α_1	α_2	α_3	α_4	α_5	α_6	α_7	α_8
Ref.	0.98	1.02	0.98	1.09	1.02	0.97	0.90	1.04
ANN	1.00	0.98	1.05	1.05	1.01	1.01	0.90	1.01

compared with the experiments and Yld2000–2d prediction using Ref. parameters in Section 4.2. Secondly, the thinning profile around the hole periphery and strain path in the HE simulations using ANN prediction of Yld2000–2d parameters is evaluated in Section 4.3.

4.2. Validation of plastic anisotropy in uniaxial tension

Fig. 4(a) shows the yield loci described by ANN and Ref. parameters. The ANN prediction (red solid line) closely aligns with Ref. (blue dashed line) yield locus and the UT and PST experiments (circular symbol), except for UT in TD, where the ANN prediction is slightly overestimated. Despite the deviation from the experiments, the ANN model effectively captures the variation of normalized stress and r-value with respect to the material orientation as shown in Figs. 4(b) and 4(c), respectively. Specifically, the ANN model shows good agreement with the Ref. and experiments within the ranges of 0° and 45° for normalized stress and 30° and 60° for r-value. Although the cause of the deviation in predictions is unclear due to the complexity of ANN structure and training, this potentially could be improved with additional ANN input variables and training data. From the comparisons of the plastic anisotropy, it can be concluded that the ANN model developed in this study can predict reasonable anisotropic parameters for the Yld2000–2d yield function using a single HE test with significantly reduced experimental effort.

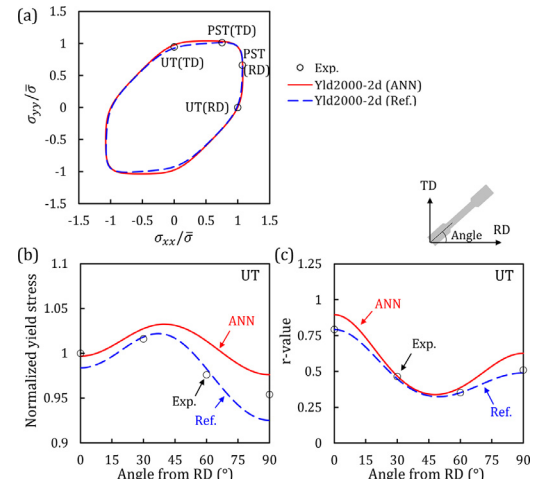


Fig. 4. Comparison of (a) yield loci, (b) normalized yield stresses, and (c) r-values from experiments and numerical simulations, from both ANN prediction and reference Yld2000–2d anisotropic parameters.

4.3. Validation of thinning prediction in HE test

HE simulations are performed with both ANN and Ref. anisotropic parameters to compare the thinning distribution. The thickness strain profiles are measured at 3 punch strokes, i.e., $U = 10$ mm (black), 13 mm (blue), and 16 mm (red) in Figs. 5(b) and (c), for 2 different initial circumferences of R18 mm (Fig. 5(b)) and R20 mm (Fig. 5(c)), corresponding to initially 0.5 mm and 2.5 mm from the hole edge as seen in Fig. 5(a). The ANN (solid line) and Ref. (dashed line) predictions capture the thinning behavior, e.g., max. thinning location and average strain level around the hole, reasonably well at both R18 mm (Fig. 5(b)) and R20 mm (Fig. 5(c)). The average deviations of thinning distributions by ANN and Ref. predictions from the experiments shown in Figs. 5(b) and 5(c) are 8.9 % and 7 %, and 8.9 % and 8.9 %, respectively. This highlights the importance of capturing the material behavior at various stress states, including PST, for accurate thinning predictions in HE [5,15], as in both ANN and Ref. cases.

The strain paths, extracted at 3 locations along the RD, DD, and TD, are also compared in Fig. 6. The experiment reveals that the strain states are changed from UT at P1 (R18 mm), to PST at P2 (R28 mm), and to biaxial tension at P3 (R35.2 mm). Strain path predictions by the ANN are closely aligned with Ref. and are comparable with the experiment (see Fig. 4(c)). This demonstrates the ability of the ANN model to predict anisotropic parameters well despite only requiring

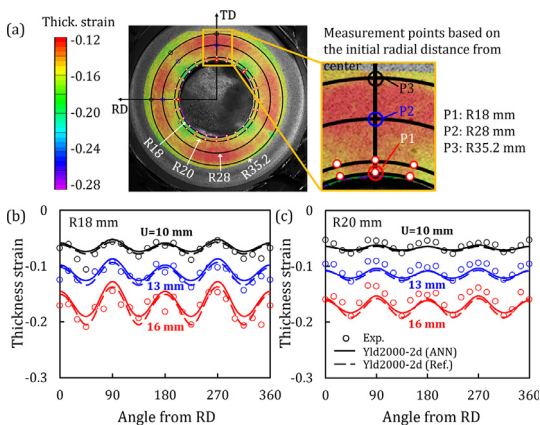


Fig. 5. Comparison of the HE experiments and simulations: (a) thickness strain contour at punch stroke $U=16$ mm and thickness strain profiles measured at (b) R18 mm and (c) R20 mm.

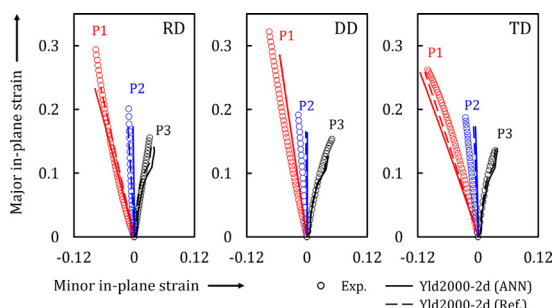


Fig. 6. Comparison of strain paths at P1, P2, and P3 along the radial directions in the RD, DD, and TD.

a single experiment compared to 3 different testing setups in the Ref. approach. A means to further validate the simulations in relation to the experiments is by comparing the punch force-stroke curves in Fig. 7. Both simulation curves are comparable with the experiment.

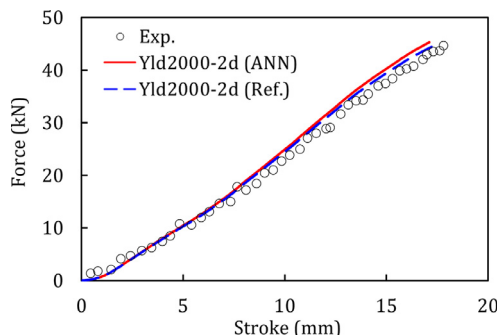


Fig. 7. Comparison of punch force-stroke curves for the experiment and simulations performed with ANN and Ref. anisotropic parameters.

5. Conclusions and future work

An ANN model to predict material parameters of the non-quadratic anisotropic yield function, Yld2000-2d, is proposed as an alternative to the conventional method, which needs at least 4 experimental tests and a numerical algorithm. A HE test is utilized due to the various stress states exhibited during the experiment. In this study, 2500 HE simulations are performed to generate a virtual training dataset using randomly selected 8 anisotropic parameters, and the 2 normal strain components at 7 different elements, including nearly UT and PST located at 0° , 45° , and 90° , corresponding to RD, DD, and TD, and nearly balanced biaxial tension at RD, are extracted from simulations. Hidden layers and nodes in the ANN architecture are optimized using Keras-Tuner and activated using a sigmoid function. The ANN model is then trained using the dataset obtained at a punch stroke of $U = 16$ mm.

The ANN model is applied to AA6022-T4 and validated by comparing plastic anisotropy in UT, i.e., normalized yield stresses and

r-values, and yield loci, as well as HE test data, including thinning variation, stain path, and punch force-stroke curve. The predictions of ANN Yld2000-2d parameters are in good agreement with the experiment and the prediction with Ref. Yld2000-2d parameters. For future work, additional training data extracted from more elements in the HE simulations and the inclusion of shear data may improve the ANN model performance.

Declaration of competing interest

The authors declare that they have no known competing financial interests or personal relationships that could have appeared to influence the work reported in this paper.

CRedit authorship contribution statement

Jinjae Kim: Methodology, Software, Validation, Formal analysis, Investigation, Data curation, Writing – original draft, Writing – review & editing, Visualization, Funding acquisition, Conceptualization, Investigation. **Abrar S. Ebrahim:** Software, Validation, Formal analysis, Investigation, Data curation, Writing – original draft, Writing – review & editing. **Brad L. Kinsey:** Funding acquisition, Resources, Writing – review & editing, Supervision. **Jinjin Ha:** Methodology, Supervision, Project administration, Conceptualization, Writing – review & editing.

Acknowledgement

This work was supported by NSF EPSCoR award #1757371.

References

- [1] Barlat F, Brem JC, Yoon JW, Chung K, Dick RE, Lege DJ, Pourboghrat, Choi S-H, Chu E (2003) Plane Stress Yield Function For Aluminum Alloy Sheets—Part 1: Theory. *International Journal of Plasticity* 19:1297–1319.
- [2] Kim J-H, Barlat F, Pierron F, Lee M-G (2014) Determination of Anisotropic Plastic Constitutive Parameters Using the Virtual Fields Method. *Experimental Mechanics* 54:1189–1204.
- [3] Ha J, Coppiepers S, Korkolis YP (2020) On The Expansion Of A Circular Hole In An Orthotropic Elastoplastic Thin Sheet. *International Journal of Mechanical Sciences* 182:105706.
- [4] Zhang S, Leotoing L, Guines D, Thullier S, Zang S (2014) Calibration Of Anisotropic Yield Criterion With Conventional Tests Or Biaxial Test. *International Journal of Mechanical Sciences* 85:142–151.
- [5] Park HS, Barlat F, Lee SY (2023) Comparison Of Anisotropic Yield Functions And Calibrations For Accurate Thickness Prediction In Hole Expansion Test. *International Journal of Materials and Product Technology* 319:118070.
- [6] Güner A, Soysalcan C, Brosius A, Tekkaya AE (2012) Characterization Of Anisotropy Of Sheet Metals Employing Inhomogeneous Strain Fields For Yld2000-2D Yield Function. *International Journal of Solids and Structures* 49:3517–3527.
- [7] Coppiepers S, Hakoyama T, Debruyne D, Takahashi S, Kuwabara T (2018) Inverse Yield Locus Identification Using A Biaxial Tension Apparatus With Link Mechanism And Displacement Fields. *Journal of Physics: Conference Series* 1063:012039.
- [8] Fu J, Zhu K, Nie X, Tang Y, Yang Z, Qi L (2021) Inertia-Based Identification Of Elastic Anisotropic Properties For Materials Undergoing Dynamic Loadings Using The Virtual Fields Method And Heterogeneous Impact Tests. *Materials & Design* 203:109594.
- [9] Zhang Y, Van Bael A, Andrade-Campos A, Coppiepers S (2022) Parameter Identifiability Analysis: Mitigating The Non-Uniqueness Issue In The Inverse Identification Of An Anisotropic Yield Function. *International Journal of Solids and Structures* 243:111543.
- [10] Rossi M, Pierron F (2012) Identification Of Plastic Constitutive Parameters At Large Deformations From Three Dimensional Displacement Fields. *Computational Mechanics* 49:53–71.
- [11] Rossi M, Pierron F, Štamborská M (2016) Application Of The Virtual Fields Method To Large Strain Anisotropic Plasticity. *International Journal of Solids and Structures* 97–98:322–335.
- [12] Wessel A, Morand L, Butz A, Helm D, Volk W (2021) A New Machine Learning Based Method For Sampling Virtual Experiments And Its Effect On The Parameter Identification For Anisotropic Yield Models. *IOP Conference Series: Materials Science and Engineering* 1157:012026.
- [13] Karadogan C, Cyron P, Liewald M (1989) Potential Use Of Machine Learning To Determine Yield Locus Parameters. *IOP Conference Series: Materials Science and Engineering* 2021(1157):012064.
- [14] Kim J, Pham QT, Kim Y (2021) Thinning Prediction Of Hole-Expansion Test For DP980 Sheet Based On A Non-Associated Flow Rule. *International journal of mechanical sciences* 191:106067.
- [15] Ha J, Korkolis YP (2021) Hole-Expansion: Sensitivity Of Failure Prediction On Plastic Anisotropy Modeling. *International Journal of Manufacturing and Material Processing* 5:28.